

COMMUNICATION

Tubulin acetylation increases cytoskeletal stiffness to regulate mechanotransduction in striated muscle

 Andrew K. Coleman^{1*}, Humberto C. Joca^{1*}, Guoli Shi², W. Jonathan Lederer¹, and Christopher W. Ward²

Microtubules tune cytoskeletal stiffness, which affects cytoskeletal mechanics and mechanotransduction of striated muscle. While recent evidence suggests that microtubules enriched in detyrosinated α -tubulin regulate these processes in healthy muscle and increase them in disease, the possible contribution from several other α -tubulin modifications has not been investigated. Here, we used genetic and pharmacologic strategies in isolated cardiomyocytes and skeletal myofibers to increase the level of acetylated α -tubulin without altering the level of detyrosinated α -tubulin. We show that microtubules enriched in acetylated α -tubulin increase cytoskeletal stiffness and viscoelastic resistance. These changes slow rates of contraction and relaxation during unloaded contraction and increased activation of NADPH oxidase 2 (Nox2) by mechanotransduction. Together, these findings add to growing evidence that microtubules contribute to the mechanobiology of striated muscle in health and disease.

Introduction

Microtubule binding to actin, intermediate filaments, and protein cytolinkers regulates cytoskeletal mechanics and mechanotransduction (Wang et al., 1993; Alenghat and Ingber, 2002; Prosser et al., 2011; Khairallah et al., 2012). Microtubule mechanotransduction through NADPH oxidase 2-dependent reactive oxygen species (ROS) was first identified in striated muscle and confirmed in disparate cell types. Evidence in striated muscle shows that disease-altered microtubules contribute to a pathological increase in cytoskeletal mechanics (Zile et al., 1999; Fassett et al., 2013; Belanto et al., 2016; Kerr et al., 2015; Prosser et al., 2011; Khairallah et al., 2012) and mechanotransduction (Kerr et al., 2015; Prosser et al., 2011; Khairallah et al., 2012), underscoring an increased susceptibility to contraction-induced injury in skeletal muscle and a predisposition to arrhythmic events in the heart (Kerr et al., 2015).

Microtubules are dynamic polymers of α - β protein dimers, with their posttranslational modification (PTM) by detyrosination (deTyrMT) or acetylation (acetylMT) increasing filament longevity and binding (Roll-Mecak, 2015; Verhey and Gaertig, 2007; Westermann and Weber, 2003; Janke and Magiera, 2020). While deTyrMT and acetylMT are evident in healthy cardiac and skeletal muscle, both are dramatically elevated in disease. Recent works have implicated deTyrMTs for regulating striated muscle myocyte mechanics and mechanotransduction and for

its excess in disease (Robison et al., 2016; Kerr et al., 2015). Despite evidence in neurons that acetylMTs are a positive regulator of cytoskeletal mechanics and mechanotransduction (Morley et al., 2016), recent work in cardiomyocytes suggests a suppressive effect (Swiatlowska et al., 2020). In any case, the independent role of α -tubulin acetylation on cellular mechanics and mechanotransduction has yet to be defined. Here, we sought to determine the independent role of acetylMTs on cytoskeletal mechanics and mechanotransduction in striated muscle.

Materials and methods

Animal models and cell preparation

Adult C57/BL6 mice (12–24 wk old) were used to isolate cardiomyocytes and flexor digitorum brevis (FDB) fibers. Cardiomyocytes were isolated using Langendorff retrograde perfusion using 1 mg/ml collagenase II (Kerr et al., 2015), and FDBs were digested overnight in 1 mg/ml collagenase A followed by gentle trituration to obtain single cells (Kerr et al., 2015). Cells were treated with 10 μ M Tubacin or vehicle (DMSO) for 2 h. In a second cohort of animals, FDBs were electroporated with pcDNA3.1 overexpression vector containing GFP (control) or α TAT-GFP 4 d before enzymatic digestion (Kerr et al., 2015).

¹Center for Biomedical Engineering and Technology, University of Maryland School of Medicine, Baltimore, MD; ²Department of Orthopedics, University of Maryland School of Medicine, Baltimore, MD.

*A.K. Coleman and H.C. Joca contributed equally to this paper; Correspondence to Humberto C. Joca: hjoca@som.umaryland.edu; Christopher W. Ward: ward@umaryland.edu

This work is part of a special collection on myofilament function and disease.

© 2021 Coleman et al. This article is distributed under the terms of an Attribution-Noncommercial-Share Alike-No Mirror Sites license for the first six months after the publication date (see <http://www.rupress.org/terms/>). After six months it is available under a Creative Commons License (Attribution-Noncommercial-Share Alike 4.0 International license, as described at <https://creativecommons.org/licenses/by-nc-sa/4.0/>).

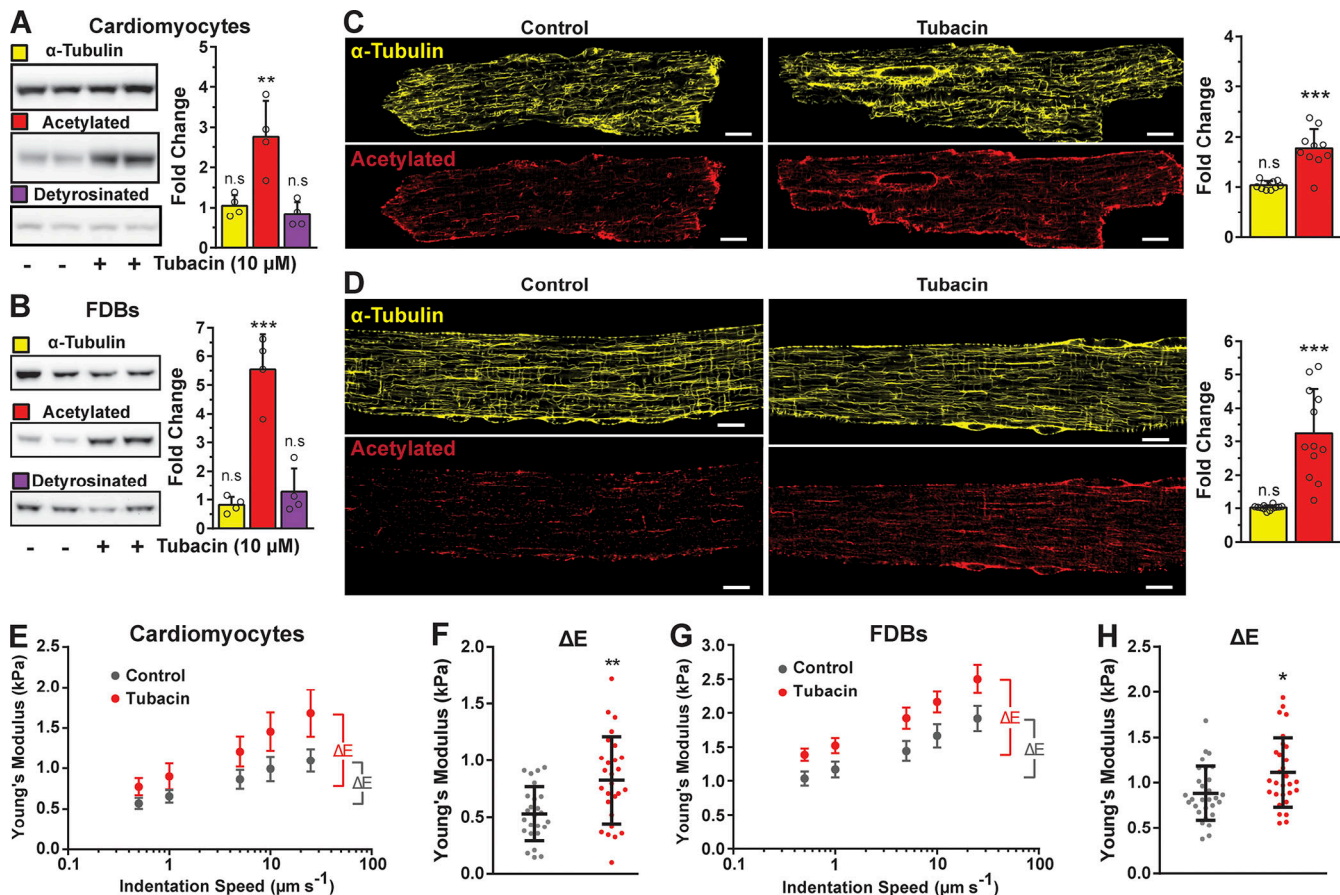


Figure 1. HDAC6 inhibition increases α -tubulin acetylation independently of altering the density of microtubules and increases cell viscoelastic resistance. (A and B) Western blot of isolated cardiomyocytes and FDB fibers treated with HDAC6 inhibitor Tubacin (10 μ M, 2 h, $n = 4$). Quantification of α -tubulin and acetylated and detyrosinated tubulin normalized to Ponceau and expressed as fold-change from control conditions (vehicle only). **(C and D)** Immunofluorescence and quantification of isolated cardiomyocytes and FDB fibers, respectively. Tubulin abundance was determined from a binary quantification normalized to cell area and expressed as fold change from control. FDB, $n = 12$; cardiomyocytes, $n = 10$. **(E-H)** Young's modulus of cardiomyocytes and FDB fibers treated with Tubacin (red) from nanoindentation at different speeds (E and G, respectively). The derived viscoelastic resistance from experiments shown in E and G is represented in F ($n = 4$; control, $n = 25$; Tubacin, $n = 27$) and H ($n = 4$; control, $n = 29$; Tubacin, $n = 29$), respectively. *, $P < 0.05$; **, $P < 0.01$; ***, $P < 0.001$; scale bars, 10 μ m.

Western blots and immunofluorescence staining

Isolated cells lysates were run on a polyacrylamide SDS gel. Protein was transferred to a nitrocellulose membrane and blocked (5% milk). The membrane was probed with primary antibodies for α -tubulin (322588, clone B-5-1-2; Thermo Fisher Scientific), acetylated (T7451, clone 6-11B-1; Sigma-Aldrich), or detyrosinated tubulin (ab48389; Abcam). Blots were then labeled with the appropriate corresponding secondary antibody and detected through chemiluminescent imaging. For immunofluorescence, FDBs or cardiomyocytes were fixed in 4% paraformaldehyde for 20 min followed by permeabilization in 0.1% Triton X-100 for 15 min. Cells were blocked in SuperBlock PBS (37515; Thermo Fisher Scientific) for 2 h. Primary antibodies were used at 1:200 overnight at 4°C. Secondary antibodies were incubated at 1:200 for 2 h. Cells were imaged with a Nikon A1R inverted confocal microscope.

Nanoindentation

FDBs or cardiomyocytes were allowed to settle on a glass-bottom dish coated with ECM (E6909; Sigma-Aldrich). Cells were

indented 1 μ m with a nanoindenter (Chiari; Optics11) using a cantilever (0.044 N/m stiffness) with round probe (3- μ m radius). Indentation speeds from 0.5 to 25 μ m/s were used to calculate the Young's modulus using the Hertzian contact model. The slowest indentation represents the elastic modulus, while the viscous modulus (ΔE) can be derived from the fastest and slowest indentation (Chen et al., 2018).

Unloaded shortening contractile kinetics

In custom-made chambers, FDBs or cardiomyocytes were paced at 1 Hz using electric field stimulation (FDBs, 600 mA, 0.2 ms; cardiomyocytes, 600 mA, 2 ms). The sarcomere length was recorded using a single-cell contractile system (Aurora Scientific), and amplitude/kinetics were calculated using a customized Matlab script.

Myocyte attachment and ROS measurements

Isolated FDB fibers were attached to microfabricated glass rod holders (IonOptix) coated with MyoTak as previously described (Kerr et al., 2015). ROS production was measured using the fluorescent indicator 5-(and-6)-carboxy-2',7'-dihydrofluorescein

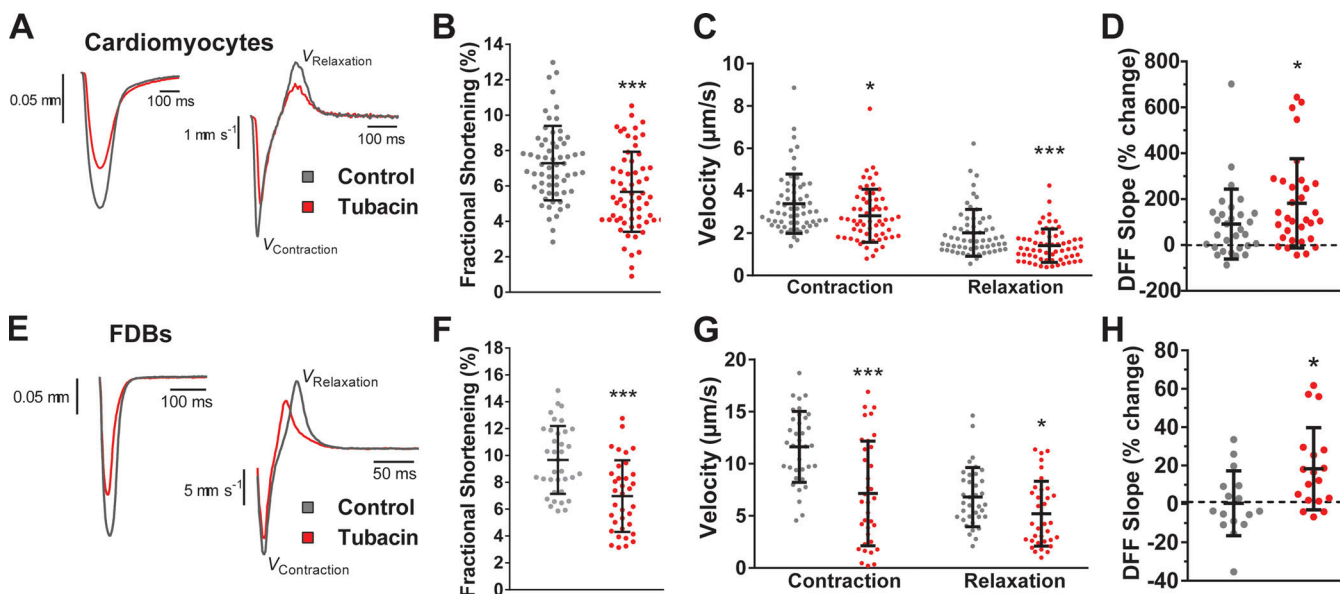


Figure 2. Increased MT acetylation slows contractile kinetics and modulates mechanosensitive ROS production. (A–C and E–G) Representative sarcomere length and velocity during contraction (A and E) treated with Tubacin (red) and respective controls (gray); measured fractional shortening (B and F) and contractile kinetics (C and G) from cardiomyocytes and FDB fibers, respectively. (D) Quantification of the change in ROS production in cardiac cells during 2-Hz stimulated contractions measured by the change in dihydrofluorescein fluorescence increase ($n = 7$; control, $n = 30$; Tubacin, $n = 31$). (H) Quantification of the change in ROS production during 2-Hz cyclic stretch in FDB fibers ($n = 3$; control, $n = 16$; Tubacin, $n = 18$). *, $P < 0.05$; ***, $P < 0.001$.

Downloaded from https://academic.oup.com/jgp/article-pdf/133/7/202012743/1802263/jgp-202012743.pdf by guest on 09 February 2020

diacetate (FDBs, 10 μ M, 40 min; cardiomyocytes, 6 μ M, 30 min; Thermo Fisher Scientific). After measuring ROS production in cells at rest, mechanical stimulation was initiated in loaded cells with a 2-Hz sinusoidal stretch waveform (10% of resting sarcomere length) imposed for 10 s (for FDBs) or 2-Hz electrical stimulation (for cardiomyocytes). Mechano-activated ROS production was derived from the increase in fluorescence during stretch/contractions normalized to the basal increase in dihydrofluorescein fluorescence.

Measurements in intact muscle

Mice were treated with the histone deacetylase 6 (HDAC6) inhibitor Tubastatin A (50 mg/kg/d) or vehicle control for 3 d. Following the treatment period, the extensor digitorum longus (EDL) was removed tendon-to-tendon and mounted in an in vitro system (Aurora 3100) to assess passive and active mechanics. After equilibration and determining optimal resting length (L_o) with twitch contractions, passive mechanics were quantified with stretches to 5, 10, 15, and 20% above L_o .

Statistics and data availability

Two-group comparison was performed using *t* test or Mann-Whitney *U* test for parametric and nonparametric datasets, respectively. The data are presented as mean \pm SD. The only exception is stiffness-indentation velocity relationship curves (Fig. 1, E and G), for which the data comparison was performed using two-way ANOVA, and data are presented as mean \pm 95% confidence interval. The data discussed here and additional experimental control datasets are available upon request.

Online supplemental material

Table S1 contains numerical data describing contraction of isolated unloaded FDBs or cardiomyocytes paced at 1 Hz using

electric field stimulation. Table S2 shows simultaneous measurement of the calcium transient (Indo 1-AM, 2 μ M for 15 min).

Results and discussion

The acetylation of α -tubulin is by α -tubulin acetyltransferase 1 (α TAT1) at K40 on a loop (residues P37 to D47; Kalebic et al., 2013; Eshun-Wilson et al., 2019) within the microtubule lumen. This modification is then reversed by HDAC6 or the NAD⁺-dependent deacetylase Sirtuin 2 (Hubbert et al., 2002; North et al., 2003). Our initial experiments used Tubacin, a pharmacologic HDAC6 inhibitor with a high specificity for HDAC6. The cytosolic localization of HDAC6 precludes a direct effect on gene expression via histone acetylation (Haggarty et al., 2003). In enzymatically isolated ventricular cardiomyocytes and FDB skeletal myofibers, we show that Tubacin increased the level of α -tubulin acetylation without altering the level of detyrosinated α -tubulin or the expression of α -tubulin protein (Fig. 1, A and B). A further examination of microtubule structure in both cell types revealed that Tubacin treatment increased the level of tubulin acetylation without altering microtubule density (Fig. 1, C and D). Using this treatment, we can accurately assess the contribution of acetylated tubulin to cellular viscoelastic resistance and microtubule-dependent mechano-signaling pathways independently of changes in detyrosinated tubulin or microtubule density.

The contribution of microtubules to the cytoskeletal stiffness and viscoelastic resistance of cardiac and skeletal myocytes is reflected in measures of their transversal stiffness and contractile kinetics (Chen et al., 2018; Kerr et al., 2015). While the level of α -tubulin modification by detyrosination has been shown to alter cytoskeletal stiffness and myocyte mechanics, the

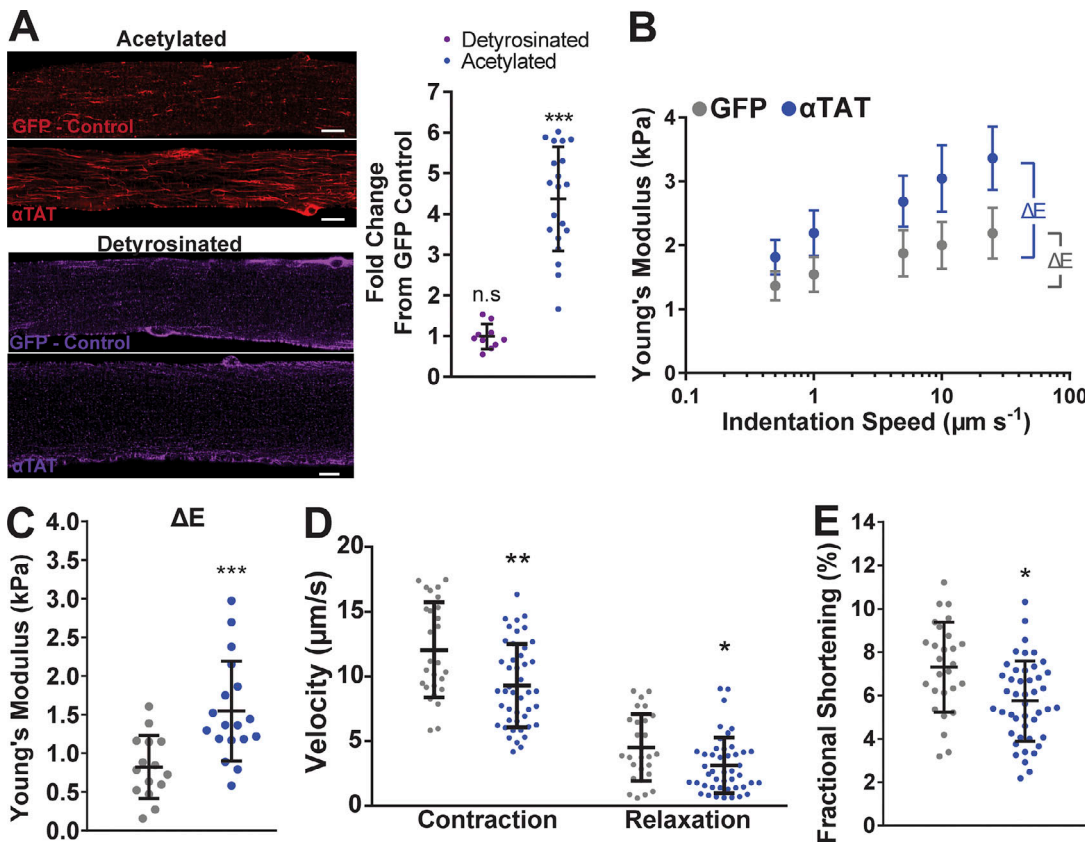


Figure 3. Overexpression of αTAT increases viscoelastic resistance and slows contractile kinetics. (A) Immunofluorescent staining and quantification of acetylated and deTyrrosinated tubulin in FDBs overexpressing αTAT (fold-change from GFP-only controls). (B and C) Young's modulus of FDB fibers overexpressing αTAT (blue) and GFP control (gray) from nanoindentation at different speeds (deTyrrosinated tubulin, $n = 10$; acetylated tubulin, $n = 20$; B) and their derived viscoelastic resistance ($n = 4$; GFP, $n = 15$; αTAT, $n = 17$; C). (D and E) Peak contraction, relaxation velocities (D), and fractional shortening (E) measured from FDB fibers overexpressing αTAT (blue) and GFP-only controls (gray). Unloaded shortening parameters ($n = 4$; GFP, $n = 27$; αTAT, $n = 45$). n.s, not significant; *, $P < 0.05$; **, $P < 0.01$; ***, $P < 0.001$; scale bars, 10 μ m.

independent effect of α-tubulin acetylation is unknown. Using measures of nanoindentation mechanics at varying speeds, we show that the Tubacol-dependent increase in acetylMTs significantly increases cellular stiffness (Fig. 1, E and G) and viscous resistance in both cardiomyocytes and FDB myofibers (Fig. 1, F and H). Aligned with these changes, we show a significant reduction in the fractional shortening (Fig. 2, B and F) and rates of both contraction and relaxation (Fig. 2, C and G) during unloaded contractions. Our profiling of unloaded shortening in conjunction with cytosolic calcium (Indo 1-AM) revealed a minimal change in calcium transient kinetics. This result reinforces the conclusion that microtubules are responsible for the altered sarcomere mechanics (Table S1 and Table S2).

Consistent with the role of microtubules in mechanotransduction (Prosser et al., 2011), we show a significant increase in mechano-elicited ROS production in single cardiomyocytes undergoing unloaded paced contraction at 2 Hz (Fig. 2 D) and in single FDBs challenged with 2 Hz cyclic passive stretch (Fig. 2 H). These results align with reports that acetylMTs are responsible for the mechanosensitive touch response in mice and *Drosophila melanogaster* (Morley et al., 2016; Yan et al., 2018), as well as evidence that acetylated α-tubulin underlies the increased resistance seen with repetitive strain to microtubules

in vitro (Portran et al., 2017; Xu et al., 2017), a property that would facilitate the transfer of energy for mechanotransduction in striated muscle (Kerr et al., 2015; Khairallah et al., 2012; Chen et al., 2018).

We used the genetic overexpression of αTAT in mouse FDB muscle as an orthogonal approach to the pharmacologic increase in tubulin acetylation. Acetylation by αTAT1 is highly specific to polymerized tubulin (Friedmann et al., 2012) and without activity toward histone proteins (Shida et al., 2010). Following enzymatic isolation of FDB myofibers, we observed an increased level of acetylMTs in fibers overexpressing αTAT versus GFP-only transfected fibers (Fig. 3 A). However, αTAT overexpression did not affect the abundance of deTyrMT, similar to HDAC6 inhibition. Measures of passive cell mechanics showed that acetylMTs increased cell stiffness and viscoelastic resistance (Fig. 3, B and C), with unloaded shortening confirming the suppressive effect on contractile kinetics (Fig. 3, D and E). These changes in sarcomere mechanics and cellular stiffness are in line with the inhibition of HDAC6, which consolidates the impact of this PTM on striated muscle function. Taken together, these results identify acetylated tubulin as a regulator of cytoskeletal stiffness and microtubule-dependent mechanotransduction in isolated FDB myofibers and cardiomyocytes.

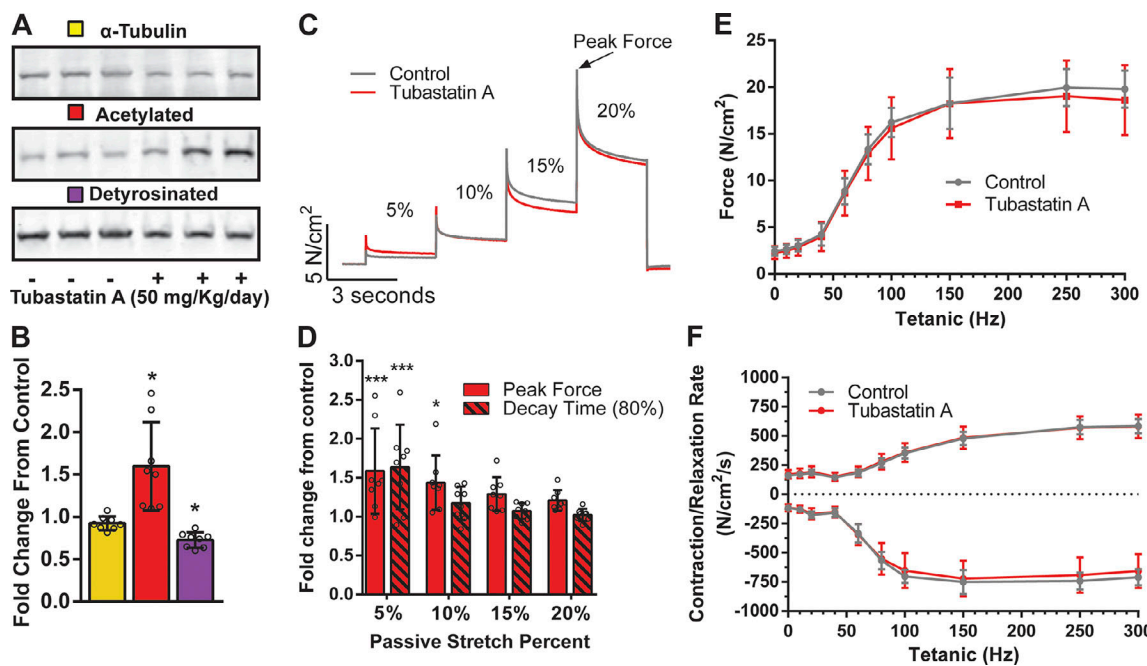


Figure 4. Microtubule acetylation has diminished impact on contractile mechanics in intact muscle. **(A)** Western blot of contralateral EDL from animals treated with Tubastatin A or vehicle control ($n = 8$). **(B)** Quantification of α -tubulin, acetylated tubulin, and detyrosinated tubulin protein expression. **(C)** Representative traces of successive stretches from intact EDL muscle in a bath. **(D)** Fold-change from control of Tubastatin A-treated animals. Quantification of peak force and decay time to 80% of peak for each successive stretch. **(E)** Force frequency curve from intact EDL muscle in a bath. **(F)** Contraction and relaxation rate from intact EDL stimulated at increasing frequencies; $n = 8$. * $P < 0.05$; *** $P < 0.001$.

Measures of sarcomere dynamics in single fibers/myocytes during unloaded contractions have been effectively used by our group and others (Robison et al., 2016; Kerr et al., 2015) to dissect the impact of microtubule PTMs as regulators of sarcomere mechanics. While it is tempting to suggest that acetylated microtubules impact the passive and active mechanics of intact muscle, the shortened sarcomere length and absence of load intrinsic to this assay diminish the ability to extrapolate these results. To address this issue directly, we treated mice *in vivo* for 3 d with the HDAC6 inhibitor Tubastatin A or vehicle control (Fig. 4, A and B). Following the treatment period, the EDL was removed tendon to tendon and mounted in an *in vitro* system (Aurora 3100) to assess passive and active mechanics. Following equilibration and determining optimal resting length (L_0) with twitch contractions, passive mechanics were quantified with stretches to 5, 10, 15, and 20% above L_0 . We show that *in vivo* Tubastatin A treatment effectively increased the level of tubulin acetylation, with minimal alteration of detyrosination. In the EDL, we show that Tubastatin A treatment increased peak passive tension at 5 and 10% stretch and increased decay time at 5%, with no effect at longer length excursions (Fig. 4, C and D). Given that 5–20% excursions from L_0 span the physiological working range reported for mouse EDL (Burkholder and Lieber, 2001), we conclude that acetylated microtubules impact the passive mechanics of muscle at low levels of sarcomere strain. This finding is consistent with titin being the dominant regulator of passive mechanics across the physiological range of sarcomere strain (Granzier and Irving, 1995; Herzog, 2014; Brynnel et al., 2018). Extending this observation, we show that Tubastatin A

treatment had no effect on the magnitude or kinetics of electrically evoked EDL contractions *in vitro* (Fig. 4, E and F).

Taking these results together, we report that α -tubulin acetylation is an independent positive regulator of the mechanics and magnitude of mechanotransduction in cardiomyocytes and skeletal muscle fibers. Given the depth and breadth of these results in striated muscle, and their qualitative alignment with results in other cell types, we found a recent report of an inverse relationship between acetylMT abundance and cardiomyocyte mechanics (Swiatlowska et al., 2020) rather surprising. However, the use of pharmacologic manipulation on the background of cardiomyopathy, and indirect measures of membrane mechanics, likely contributed to the contradiction with our current results. Furthermore, the strength of our findings is bolstered by measures of passive nanoindentation, active sarcomere mechanics, and mechanotransduction-dependent ROS signaling, three outcome measures formerly shown to be effective by our group and others (Kerr et al., 2015; Chen et al., 2018). A further strength is the quantitative similarity of our results across mechanistically distinct means of increasing α -tubulin acetylation (i.e., HDAC6 inhibition versus α TAT1 overexpression). Finally, our results were highly specific to α -tubulin acetylation and occurred independently of alterations in MT density or levels of deTyrMT in both cardiac and skeletal striated muscle.

We take these results as an extension of our discovery that tubulin PTMs alter microtubule properties that regulate cytoskeletal mechanics and tune the magnitude of striated muscle mechanotransduction. Our current findings on acetylated

α -tubulin, and our works and others on deetyrosinated α -tubulin, propose each PTM to be an independent regulator of microtubule properties, yet both result in increased cytoskeletal mechanics and mechanotransduction in striated muscle. The deetyrosinated α -tubulin C-terminal tail promoting microtubule binding to desmin is the proposed mechanism of how deTyrMTs regulate sarcomere mechanics and mechanotransduction. Alternatively, acetylated α -tubulin is proposed to promote microtubule stability by weakening lateral contacts of microtubule protofilaments (Eshun-Wilson et al., 2019). As both PTMs are elevated in diseased striated muscle, we hypothesize that each acts independently toward the pathological increase in mechanics and mechanotransduction. Given that a targeted reduction of deTyrMTs effectively reduces cellular and tissue pathology (Chen et al., 2020; Robison et al., 2016; Kerr et al., 2015; Chen et al., 2018), we posit that targeting HDAC6 or α TAT may expand our opportunity toward normalizing these pathological changes in diseased striated muscle.

Acknowledgments

Henk L. Granzier served as editor.

This research was supported by the American Heart Association (grant 19POST34450156 to H.C. Joca) and the National Institutes of Health (grants T32-AR007592-23 to A.K. Coleman, U01-HL116321 to W.J. Lederer, R01-HL142290 to W.J. Lederer and C.W. Ward, and R01-AR071618 and R01-AR071614 to C.W. Ward).

The authors declare no competing financial interests.

Author contributions: A.K. Coleman, H.C. Joca, G. Shi., and C.W. Ward designed and conducted experiments. Results were analyzed and interpreted by A.K. Coleman, H.C. Joca, C.W. Ward, and W.J. Lederer. The manuscript was written by A.K. Coleman, H.C. Joca, and C.W. Ward, and edited and finalized by all authors.

Submitted: 14 August 2020

Revised: 29 January 2021

Accepted: 1 March 2021

References

Alenghat, F.J., and D.E. Ingber. 2002. Mechanotransduction: all signals point to cytoskeleton, matrix, and integrins. *Sci. STKE*. 2002:pe6. <https://doi.org/10.1126/stke.2002.119.pe6>

Belanto, J.J., J.T. Olthoff, T.L. Mader, C.M. Chamberlain, D.M. Nelson, P.M. McCourt, D.M. Talsness, G.G. Gunderson, D.A. Lowe, and J.M. Ervasti. 2016. Independent variability of microtubule perturbations associated with dystrophinopathy. *Hum. Mol. Genet.* 25:4951–4961. <https://doi.org/10.1093/hmg/ddw318>

Brynnel, A., Y. Hernandez, B. Kiss, J. Lindqvist, M. Adler, J. Kolb, R. van der Pijl, J. Gohlke, J. Strom, J. Smith, et al. 2018. Downsizing the molecular spring of the giant protein titin reveals that skeletal muscle titin determines passive stiffness and drives longitudinal hypertrophy. *eLife*. 7: e40532. <https://doi.org/10.7554/eLife.40532>

Burkholder, T.J., and R.L. Lieber. 2001. Sarcomere length operating range of vertebrate muscles during movement. *J. Exp. Biol.* 204:1529–1536.

Chen, C.Y., M.A. Caporizzo, K. Bedi, A. Vite, A.I. Bogush, P. Robison, J.G. Heffler, A.K. Salomon, N.A. Kelly, A. Babu, et al. 2018. Suppression of deetyrosinated microtubules improves cardiomyocyte function in human heart failure. *Nat. Med.* 24:1225–1233. <https://doi.org/10.1038/s41591-018-0046-2>

Chen, C.Y., A.K. Salomon, M.A. Caporizzo, S. Curry, N.A. Kelly, K. Bedi, A.I. Bogush, E. Krämer, S. Schlossarek, P. Janiak, et al. 2020. Depletion of Vasohibin 1 Speeds Contraction and Relaxation in Failing Human Cardiomyocytes. *Circ. Res.* 127:e14–e27. <https://doi.org/10.1161/CIRCRESAHA.119.315947>

Eshun-Wilson, L., R. Zhang, D. Portran, M.V. Nachury, D.B. Toso, T. Löhr, M. Vendruscolo, M. Bonomi, J.S. Fraser, and E. Nogales. 2019. Effects of α -tubulin acetylation on microtubule structure and stability. *Proc. Natl. Acad. Sci. USA*. 116:10366–10371. <https://doi.org/10.1073/pnas.1900441116>

Fassett, J.T., X. Hu, X. Xu, Z. Lu, P. Zhang, Y. Chen, and R.J. Bache. 2013. AMPK attenuates microtubule proliferation in cardiac hypertrophy. *Am. J. Physiol. Heart Circ. Physiol.* 304:H749–H758. <https://doi.org/10.1152/ajpheart.00935.2011>

Friedmann, D.R., A. Aguilar, J. Fan, M.V. Nachury, and R. Marmorstein. 2012. Structure of the α -tubulin acetyltransferase, α TAT1, and implications for tubulin-specific acetylation. *Proc. Natl. Acad. Sci. USA*. 109: 19655–19660. <https://doi.org/10.1073/pnas.1209357109>

Granzier, H.L., and T.C. Irving. 1995. Passive tension in cardiac muscle: contribution of collagen, titin, microtubules, and intermediate filaments. *Biophys. J.* 68:1027–1044. [https://doi.org/10.1016/S0006-3495\(95\)80278-X](https://doi.org/10.1016/S0006-3495(95)80278-X)

Haggarty, S.J., K.M. Koeller, J.C. Wong, C.M. Grozinger, and S.L. Schreiber. 2003. Domain-selective small-molecule inhibitor of histone deacetylase 6 (HDAC6)-mediated tubulin deacetylation. *Proc. Natl. Acad. Sci. USA*. 100:4389–4394. <https://doi.org/10.1073/pnas.0430973100>

Herzog, W. 2014. The role of titin in eccentric muscle contraction. *J. Exp. Biol.* 217:2825–2833. <https://doi.org/10.1242/jeb.099127>

Hubbert, C., A. Guardiola, R. Shao, Y. Kawaguchi, A. Ito, A. Nixon, M. Yoshida, X.F. Wang, and T.P. Yao. 2002. HDAC6 is a microtubule-associated deacetylase. *Nature*. 417:455–458. <https://doi.org/10.1038/417455a>

Janke, C., and M.M. Magiera. 2020. The tubulin code and its role in controlling microtubule properties and functions. *Nat. Rev. Mol. Cell Biol.* 21: 307–326. <https://doi.org/10.1038/s41580-020-0214-3>

Kalebic, N., S. Sorrentino, E. Perlas, G. Bolasco, C. Martinez, and P.A. Hepsenstall. 2013. α TAT1 is the major α -tubulin acetyltransferase in mice. *Nat. Commun.* 4:1962. <https://doi.org/10.1038/ncomms2962>

Kerr, J.P., P. Robison, G. Shi, A.I. Bogush, A.M. Kempema, J.K. Hexum, N. Bocerra, D.A. Harki, S.S. Martin, R. Raiteri, et al. 2015. Deetyrosinated microtubules modulate mechanotransduction in heart and skeletal muscle. *Nat. Commun.* 6:8526. <https://doi.org/10.1038/ncomms9526>

Khairallah, R.J., G. Shi, F. Sbrana, B.L. Prosser, C. Borroto, M.J. Mazaitis, E.P. Hoffman, A. Mahurkar, F. Sachs, Y. Sun, et al. 2012. Microtubules underlie dysfunction in duchenne muscular dystrophy. *Sci. Signal.* 5:ra56. <https://doi.org/10.1126/scisignal.2002829>

Morley, S.J., Y. Qi, L. Iovino, L. Andolfi, D. Guo, N. Kalebic, L. Castaldi, C. Tischer, C. Portulano, G. Bolasco, et al. 2016. Acetylated tubulin is essential for touch sensation in mice. *eLife*. 5:e20813. <https://doi.org/10.7554/eLife.20813>

North, B.J., B.L. Marshall, M.T. Borra, J.M. Denu, and E. Verdin. 2003. The human Sir2 ortholog, SIRT2, is an NAD⁺-dependent tubulin deacetylase. *Mol. Cell.* 11:437–444. [https://doi.org/10.1016/S1097-2765\(03\)00038-8](https://doi.org/10.1016/S1097-2765(03)00038-8)

Portran, D., L. Schaedel, Z. Xu, M. Théry, and M.V. Nachury. 2017. Tubulin acetylation protects long-lived microtubules against mechanical ageing. *Nat. Cell Biol.* 19:391–398. <https://doi.org/10.1038/ncb3481>

Prosser, B.L., C.W. Ward, and W.J. Lederer. 2011. X-ROS signaling: rapid mechano-chemo transduction in heart. *Science*. 333:1440–1445. <https://doi.org/10.1126/science.1202768>

Robison, P., M.A. Caporizzo, H. Ahmadzadeh, A.I. Bogush, C.Y. Chen, K.B. Margulies, V.B. Shenoy, and B.L. Prosser. 2016. Deetyrosinated microtubules buckle and bear load in contracting cardiomyocytes. *Science*. 352:aaf0659. <https://doi.org/10.1126/science.aaf0659>

Roll-Mecak, A. 2015. Intrinsically disordered tubulin tails: complex tuners of microtubule functions? *Semin. Cell Dev. Biol.* 37:11–19. <https://doi.org/10.1016/j.semcdb.2014.09.026>

Shida, T., J.G. Cueva, Z. Xu, M.B. Goodman, and M.V. Nachury. 2010. The major alpha-tubulin K40 acetyltransferase alphaTAT1 promotes rapid ciliogenesis and efficient mechanosensation. *Proc. Natl. Acad. Sci. USA*. 107:21517–21522. <https://doi.org/10.1073/pnas.1013728107>

Swiatlowska, P., J.L. Sanchez-Alonso, P.T. Wright, P. Novak, and J. Gorelik. 2020. Microtubules regulate cardiomyocyte transversal Young's modulus. *Proc. Natl. Acad. Sci. USA*. 117:2764–2766. <https://doi.org/10.1073/pnas.1917171111>

Verhey, K.J., and J. Gaertig. 2007. The tubulin code. *Cell Cycle*. 6:2152–2160. <https://doi.org/10.4161/cc.6.17.4633>

Wang, N., J.P. Butler, and D.E. Ingber. 1993. Mechanotransduction across the cell surface and through the cytoskeleton. *Science*. 260:1124–1127. <https://doi.org/10.1126/science.7684161>

Westermann, S., and K. Weber. 2003. Post-translational modifications regulate microtubule function. *Nat. Rev. Mol. Cell Biol.* 4:938–948. <https://doi.org/10.1038/nrm1260>

Xu, Z., L. Schaedel, D. Portran, A. Aguilar, J. Gaillard, M.P. Marinkovich, M. Théry, and M.V. Nachury. 2017. Microtubules acquire resistance from mechanical breakage through intraluminal acetylation. *Science*. 356: 328–332. <https://doi.org/10.1126/science.aai8764>

Yan, C., F. Wang, Y. Peng, C.R. Williams, B. Jenkins, J. Wildonger, H.-J. Kim, J.B. Perr, J.C. Vaughan, M.E. Kern, et al. 2018. Microtubule Acetylation Is Required for Mechanosensation in *Drosophila*. *Cell Rep.* 25: 1051–1065.e6. <https://doi.org/10.1016/j.celrep.2018.09.075>

Zile, M.R., M. Koide, H. Sato, Y. Ishiguro, C.H. Conrad, J.M. Buckley, J.P. Morgan, and G. Cooper IV. 1999. Role of microtubules in the contractile dysfunction of hypertrophied myocardium. *J. Am. Coll. Cardiol.* 33: 250–260. [https://doi.org/10.1016/S0735-1097\(98\)00550-6](https://doi.org/10.1016/S0735-1097(98)00550-6)

Supplemental material

Two tables are provided online as Word files. Table S1 lists contraction kinetic parameters based on sarcomere length. Table S2 lists calcium transient kinetic parameters.